

Complexation-Induced Control of Electron Propagation Based on Bounded Diffusion through Nanopore-Tethered Ferrocenes

Feng Li[†] and Takashi Ito*

Department of Chemistry, Kansas State University, 213 CBC Building, Manhattan, Kansas 66506-0401, United States

S Supporting Information

ABSTRACT: This paper reports complexation-induced control of electron propagation based on bounded diffusion through ferrocene moieties that are covalently tethered onto nanopores (19 or 24 nm in diameter) derived from cylinder-forming polystyrene–poly(methylmethacrylate) diblock copolymers. The nanopores are oriented vertically and attach to a gold surface, and thus allow a faradaic current originating from the bounded diffusion to be measured using cyclic voltammetry. Such faradaic current decreases with increasing concentration of β -cyclodextrin (β -CD) in an aqueous solution, and recovers upon addition of excess 1-adamantanol as a competitive guest to the solution. These observations indicate that electron propagation can be reversibly inhibited by the formation of an inclusion complex with the surface-tethered redox moieties. Interestingly, the decrease in faradaic current is observed at an unexpectedly low β -CD concentration (ca. 1×10^{-7} M) due to the enhanced partition of β -CD into the nanopores. These results will lead to designing highly sensitive molecular switches and electrochemical sensors based on the control of bounded diffusion by the host–guest chemistry of nanopore-tethered redox moieties.

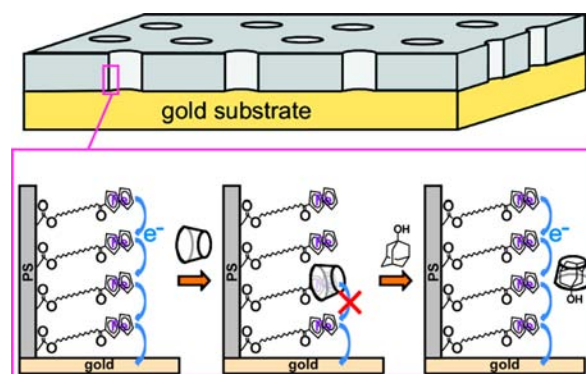
Electron hopping is a charge-transport mechanism involving an electron self-exchange reaction between adjacent, localized redox moieties that are covalently or electrostatically tethered onto a low-conductivity framework.^{1–3} If redox sites are tethered onto an immobile framework and their spacing is larger than the electron-transfer distance, electron propagation is induced by collisions between neighboring redox sites having limited mobility (bounded diffusion).⁴ Bounded diffusion plays important roles in electron transport within redox polymers employed as mediators for enzyme-based electrochemical sensors,⁵ charge propagation through surface-immobilized dye molecules in dye-sensitized solar cells,⁶ and electron conduction in molecular electronics.^{7,8} Well-defined control of the electron propagation is required in order to develop materials and devices suitable for these applications.

Electron propagation based on bounded diffusion is often assessed from an apparent diffusion coefficient (D_{ap}) measured using electrochemical methods.^{1–3} According to theoretical studies, D_{ap} is controlled by the density, electron self-exchange rate constant, electron-transfer distance, and physical displacement range of redox sites.^{4,9} The density and rate constant effects on D_{ap} have been systematically investigated for redox

polymers,¹⁰ Langmuir–Blodgett films of redox amphiphiles,¹¹ redox site-coated metal oxide surfaces,¹² and monolayer-tethered silicon surfaces.⁸ Redox site density is the parameter that is usually optimized to gain electron propagation efficiency suitable for the aforementioned applications.

Recently, we experimentally demonstrated a possibility to control bounded diffusion by the physical displacement range of surface-tethered redox moieties (Scheme 1, lower-left).¹³

Scheme 1



Hydroxy-terminated ferrocene derivatives with different alkyl chains were covalently immobilized via esterification onto the surfaces of insulator-based nanoporous films (24 nm in pore diameter, 30 nm thick)¹⁴ that were derived from a cylinder-forming polystyrene–poly(methylmethacrylate) diblock copolymer (CF-PS-*b*-PMMA).^{15,16} The nanopores were vertically oriented and directly contacted to an underlying gold substrate,¹⁷ and thus electron propagation through the tethered ferrocenes could be measured as a faradaic current using cyclic voltammetry (CV). The average spacing between adjacent redox moieties (ca. 1.2 nm), which was determined by the surface –COOH density of the native nanopores and surface reaction yield,¹⁴ was larger than the size of ferrocene (ca. 0.66 nm in diameter).¹⁸ Thus, a relatively long alkyl linker was required for the collision-induced electron propagation.¹³ In addition, electron propagation was more efficient for the longer linker, as shown by the larger D_{ap} and maximum electron propagation distance (h).¹³ These results will lead to designing unique electrochemical sensors and molecular devices that are operated based on changes in the dynamic properties of tethered redox sites.

Received: July 9, 2013

Published: October 22, 2013

In this paper, we report another approach to the control of electron propagation through nanopore-tethered redox sites. Specifically, the approach takes advantage of the complexation of ferrocene with β -cyclodextrin (β -CD).^{19,20} We have hypothesized that electron propagation through tethered ferrocenes can be inhibited by the formation of an inclusion complex with β -CD, as reported for the redox reaction of ferrocenylthiol monolayers,²¹ that of ferrocenes in aqueous solutions,^{22,23} and that of dissolved ferrocenes at β -CD monolayer-coated electrodes.²⁴ The chemical equilibrium process^{19,25} will make it possible to reversibly control the electron propagation by adjusting the concentrations of β -CD and a competitive guest species. The nanopore with a relatively large diameter (19 or 24 nm) and short length (ca. 30 nm) will offer a diffusion pathway for these molecules into the nanopores,²⁶ leading to quick complexation-induced changes in electron propagation efficiency. Interestingly, the inhibition of electron propagation is observed at a very low β -CD concentration as compared with that expected from the complex formation constants between β -CD in aqueous solutions and ferrocene moieties in a monolayer.²¹ These results indicate that the complexation-induced control of bounded diffusion through nanopore-anchored redox sites provides a unique means to design highly sensitive devices for electrochemical sensors and molecular electronic devices.^{20,27}

Nanoporous films (ca. 30 nm thick) derived from CF-PS-*b*-PMMA (Polymer Source) were prepared on gold-coated silicon substrates (LGA thin films) according to a procedure involving spin-coating of the polymer, annealing at 170 °C under vacuum, UV irradiation, and acetic acid treatment.^{13,14} In this study, 57K CF-PS-*b*-PMMA ($M_n = 39\,800$ g/mol for PS and 17 000 g/mol for PMMA) and 71K CF-PS-*b*-PMMA ($M_n = 48\,000$ g/mol for PS and 23 000 g/mol for PMMA) were employed to prepare thin films comprising cylindrical nanopores with diameters of 19 and 24 nm, respectively.²⁸ The resulting nanopore surface was modified via the esterification of the surface -COOH groups with 16-hydroxy-1-oxohexadecylferrocene (FcCO(CH₂)₁₅OH) using oxalyl chloride (Acros).¹⁴ Table 1 summarizes the density of ferrocene moieties on the nanopore surface (Γ) estimated using a cation-exchange method with Rhodamine 6G.¹⁴ CV measurements were carried out in a three-electrode cell using a CH Instruments model

Table 1. Surface Ferrocene Density (Γ), Apparent Diffusion Coefficients (D_{ap}), and Maximum Electron Propagation Distances (h) Measured at CF-PS-*b*-PMMA-Derived Nanoporous Films Modified with FcCO(CH₂)₁₅OH

CF-PS- <i>b</i> -PMMA	Γ (mol/cm ²) ^a	D_{ap} (cm ² /s) ^b	h (nm) ^b
71K (24 nm in pore dia.)	$(1.33 \pm 0.10) \times 10^{-10}$	$(2.3 \pm 0.7) \times 10^{-12}$	7.3 ± 1.3
57K (19 nm in pore dia.)	$(1.14 \pm 0.23) \times 10^{-10}$	$(2.4 \pm 0.9) \times 10^{-13}$	2.5 ± 0.5

^aThe average and standard deviation of Γ measured on three different samples. The values were taken from our previous reports. ^bThe average and standard deviation obtained from three different samples. The D_{ap} and h values were determined from CV data measured at different scan rates according to the method reported previously.⁹ Note that the values for 71K CF-PS-*b*-PMMA-derived nanopores were very close to those previously reported for nanopores prepared from the same block copolymer.¹³ The h values smaller than the film thickness (ca. 30 nm) suggest that not all the ferrocene moieties can react via bounded diffusion.¹³

618B electrochemical analyzer, as reported previously.¹³ All the CV data were measured in aqueous solutions containing 0.1 M NaBF₄ (Acros) at room temperature (ca. 20 °C). The concentrations of β -CD (Acros) and 1-adamantanol (AdOH, Acros) were altered by adding stock solutions (3 mM and lower concentrations for β -CD; 3 mM for AdOH) to a sample solution.

Figure 1 shows CV data measured for a ferrocene-decorated nanoporous film derived from 71K CF-PS-*b*-PMMA (24 nm in

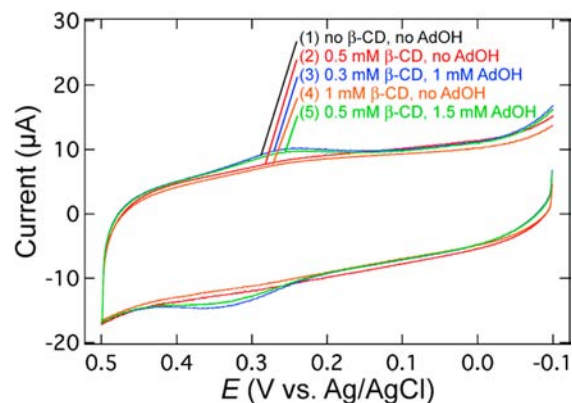


Figure 1. Cyclic voltammograms (scan rate, 0.5 V/s) measured for a gold-supported nanoporous film (24 nm in pore diameter) modified with FcCO(CH₂)₁₅OH in aqueous 0.1 M NaBF₄ containing (1) neither β -CD nor AdOH; (2) 0.50 mM β -CD; (3) 0.30 mM β -CD and 1.0 mM AdOH; (4) 1.0 mM β -CD; and (5) 0.50 mM β -CD and 1.5 mM AdOH. All the data were recorded at room temperature (ca. 20 °C).

pore diameter). A voltammogram measured in 0.1 M NaBF₄ with no β -CD (black, (1)) shows faradaic peaks around +0.25 and +0.35 V (vs Ag/AgCl) that originate from electron propagation through the nanopore-tethered ferrocenes, as reported previously.¹³ The faradaic currents drastically decreased upon addition of β -CD (0.50 mM) to the solution (red, (2)). The current decrease resulted from the inhibition of electron propagation, reflecting a decrease in the electron self-exchange rate constant between ferrocene and ferrocenium by the formation of an inclusion complex with β -CD (Scheme 1, lower-center).²³ This explanation is supported by current recovery observed after the addition of excess AdOH as a competitive guest species to the solution (blue, (3)). The recovery is attributable to the detachment of β -CD from nanopore-tethered ferrocene as a result of the formation of a more stable complex with AdOH in the solution (Scheme 1, lower-right). Indeed, the complex of β -CD with 1-adamantanecarboxylate in an aqueous solution was reported to be 5 times more stable than that with ferrocenecarboxylate.²⁹ The current decrease and recovery was observed repeatedly, as indicated by CV data measured after replacing the β -CD-AdOH mixture with 1.0 mM β -CD (orange, (4)) and upon the subsequent addition of excess AdOH to the solution (green, (5)).

The current decrease was dependent on β -CD concentration and was also observed for ferrocenes tethered to smaller nanopores. Figure 2a,b shows CV data measured for ferrocene-decorated nanoporous films derived from 71K CF-PS-*b*-PMMA (24 nm in pore diameter) and 57K CF-PS-*b*-PMMA (19 nm in pore diameter), respectively, at different β -CD concentrations. The faradaic currents observed at 0 M β -CD for the 19 nm

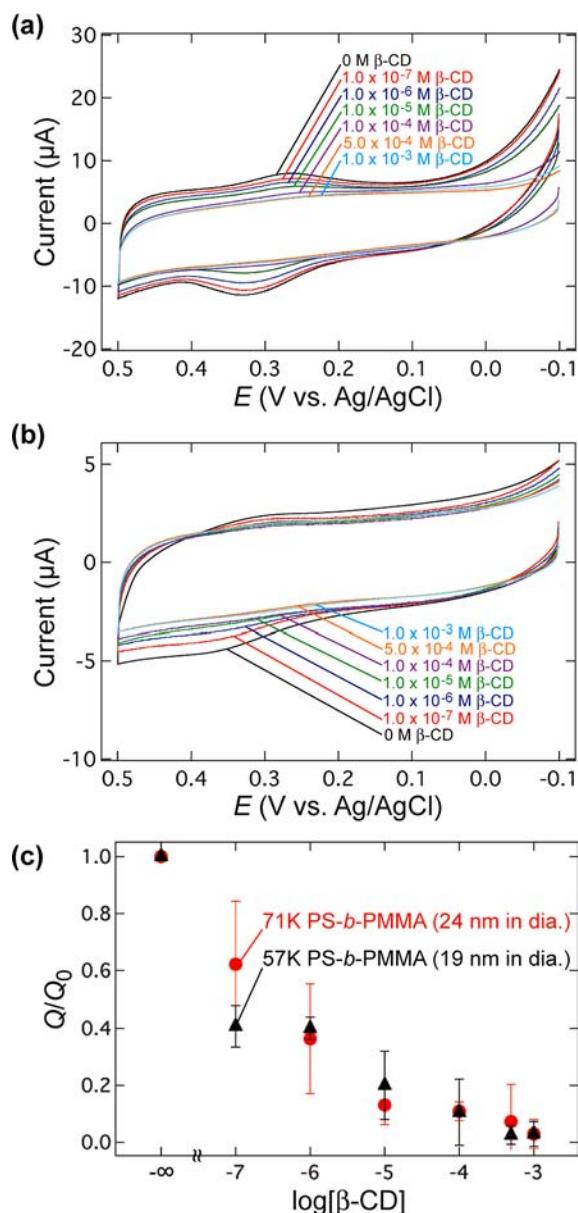


Figure 2. (a,b) Cyclic voltammograms (scan rate, 0.25 V/s) measured for gold-supported, FcCO(CH₂)₁₅OH-decorated nanoporous films derived from (a) 71K CF-PS-*b*-PMMA (24 nm in pore diameter) and (b) 57K CF-PS-*b*-PMMA (19 nm in pore diameter) at different β-CD concentrations in aqueous 0.1 M NaBF₄. Recorded at room temperature (ca. 20 °C). (c) Relationship between anodic charge ratio (Q/Q_0 ; Q_0 is the anodic charge measured in the absence of β-CD) and β-CD concentration for FcCO(CH₂)₁₅OH-decorated nanoporous films derived from 71K (red circles) and 57K CF-PS-*b*-PMMA (black triangles). The error bars represent the standard deviations of the data measured from three different samples.

nanopores were significantly smaller (Figure 2b) than for the 24 nm nanopores (Figure 2a). The smaller current reflects the lower electron propagation efficiency, as indicated by the smaller D_{ap} and h , probably due to the lower surface ferrocene density (Table 1). More importantly, both samples exhibited gradual decreases in faradaic current with increasing β-CD concentration in the range from 1.0×10^{-7} to 1.0×10^{-4} M. The β-CD concentration dependence is plausible in terms of the aforementioned mechanism based on the inhibition of

electron propagation induced by the formation of the inclusion complex, as illustrated in Scheme 1.

Figure 2c summarizes anodic charges measured for ferrocene-decorated nanopores with diameters of 24 and 19 nm at different β-CD concentrations. Here, the anodic charge (Q) is normalized by that measured at 0 M β-CD (Q_0) to compensate for variations in open pore density between different samples.¹³ Figure 2c indicates the reproducible observation of the complexation-induced current decrease at the β-CD concentration of 10^{-7} M. The current decrease at such a low β-CD concentration was unexpected, considering the complexation constant between β-CD in an aqueous solution and ferrocenylthiol monolayers ($K = 3.6 \times 10^4 \text{ M}^{-1}$).²¹ The observation of the current decrease at such a low β-CD concentration can mainly be attributed to the enhanced partition of β-CD into the hydrophobic nanopores, which leads to the higher β-CD concentration within the nanopores than in the solution bulk: Without taking the enhanced partition into account, very few nanopores (e.g., 0.06% for 20 nm diameter, 30 nm long nanopores ($9.4 \times 10^{-18} \text{ cm}^3$ in volume)) are expected to hold one β-CD molecule at 0.1 μM, and thus will be insufficient to observe the significant current decrease as shown in Figures 1 and 2. The partition may be enhanced because of the more hydrophobic environment within the nanopores, the high local concentration of the surface-tethered guests (ca. $1 \times 10^{-10} \text{ mol/cm}^2$; Table 1), and the enhanced molecule–nanopore interactions due to the enhanced molecular collisions with the nanopore wall.^{30,31} In addition, the electron hopping efficiency is very sensitive to subtle changes in dynamic properties, as suggested by the linker length dependence of D_{ap} and h ,¹³ and also in the surface density of the redox moieties, as suggested by the difference in D_{ap} and h for the two nanopores (Table 1). Such characteristics of the electron hopping may also contribute to the observation of the current reduction at the unexpectedly low β-CD concentration.

It should be noted that the Langmuir isotherm, which was used to study complexation of surface-immobilized ferrocenes,^{21,24} was not applicable for quantitative discussion of our results, as the current change was observed over the wide range (3 orders of magnitude) of β-CD concentration. The inapplicability of the Langmuir isotherm suggests that the efficiency of the current inhibition depend on the position of the complexation: As illustrated in Scheme 1, the inhibition may be more efficient if a ferrocene closer to the electrode forms the inclusion complex. Further investigations are necessary to thoroughly understand the mechanisms behind the complexation-induced inhibition of electron propagation through nanopore-anchored ferrocenes.

In summary, this Communication reports the reversible control of electron propagation through nanopore-tethered ferrocenes based on the complexation with β-CD. Such electron propagation could be inhibited by the formation of an inclusion complex between tethered ferrocenes and β-CD, and be recovered by the addition of excess AdOH as a competitive guest species for β-CD. Importantly, the inhibition of electron propagation was observed at an unexpectedly low β-CD concentration, mainly due to the enhanced partition of β-CD into the hydrophobic nanopores decorated with ferrocene moieties at a high surface concentration. The complexation-based control of electron propagation through nanopore-tethered redox moieties will thus provide a unique means for designing highly sensitive electrochemical sensors and molec-

ular devices.^{20,27} More detailed and quantitative investigations are currently ongoing in our research group for better understanding of the characteristics of such electron propagation.

■ ASSOCIATED CONTENT

📄 Supporting Information

Details of the experimental procedures. This material is available free of charge via the Internet at <http://pubs.acs.org>.

■ AUTHOR INFORMATION

Corresponding Author

ito@ksu.edu

Present Address

[†]Department of Chemistry and Biochemistry, University of Texas at Austin, Austin, Texas 78712, USA

Notes

The authors declare no competing financial interest.

■ ACKNOWLEDGMENTS

This work was mainly supported by the Division of Chemical Sciences, Geosciences, and Biosciences, Office of Basic Energy Sciences of the U.S. Department of Energy (DE-FG02-12ER16095). The authors also acknowledge ACS Petroleum Research Funds (ACS PRF #46192-G5), Terry C. Johnson Center for Basic Cancer Research and Targeted Excellence Funds of Kansas State University for partial financial support of this work.

■ REFERENCES

- (1) Majda, M. In *Molecular Design of Electrode Surfaces*; Murray, R. W., Ed.; John Wiley & Sons: New York, 1992; pp 159–206.
- (2) Andrieux, C. P.; Saveant, J.-M. In *Molecular Design of Electrode Surfaces*; Murray, R. W., Ed.; John Wiley & Sons: New York, 1992; pp 207–270.
- (3) Terrill, R. H.; Murray, R. W. In *Molecular Electronics: A 'Chemistry for the 21st Century' Monograph*; Jortner, J., Ratner, M., Eds.; Blackwell Science: Malden, MA, 1997; pp 215–239.
- (4) Blauch, D. N.; Saveant, J.-M. *J. Am. Chem. Soc.* **1992**, *114*, 3323–3332.
- (5) Heller, A. *J. Phys. Chem.* **1992**, *96*, 3579–3587.
- (6) Ardo, S.; Meyer, G. J. *Chem. Soc. Rev.* **2009**, *38*, 115–164.
- (7) McCreery, R. L.; Yan, H.; Bergren, A. *J. Phys. Chem. Chem. Phys.* **2013**, *15*, 1065–1081.
- (8) Fabre, B. *Acc. Chem. Res.* **2010**, *43*, 1509–1518.
- (9) Amatore, C.; Bouret, Y.; Maisonhaute, E.; Goldsmith, J. L.; Abruna, H. D. *Chem.–Eur. J.* **2001**, *7*, 2206–2226.
- (10) Murray, R. W. *Annu. Rev. Mater. Sci.* **1984**, *14*, 145–169.
- (11) Majda, M. In *Modified Electrodes*; Fujihira, M., Rubinstein, I., Rusling, J. F., Eds.; Wiley-VCH Verlag GmbH & Co.: Weinheim, 2007; Vol. 10, pp 211–235.
- (12) Bonhote, P.; Gogniat, E.; Tingry, S.; Barbe, C.; Vlachopoulos, N.; Lenzmann, F.; Comte, P.; Gratzel, M. *J. Phys. Chem. B* **1998**, *102*, 1498–1507.
- (13) Li, F.; Pandey, B.; Ito, T. *Langmuir* **2012**, *28*, 16496–16500.
- (14) Li, F.; Diaz, R.; Ito, T. *RSC Adv.* **2011**, *1*, 1732–1736.
- (15) Thurn-Albrecht, T.; Steiner, R.; DeRouchey, J.; Stafford, C. M.; Huang, E.; Bal, M.; Tuominen, M.; Hawker, C. J.; Russell, T. P. *Adv. Mater.* **2000**, *12*, 787–791.
- (16) Jeoung, E.; Galow, T. H.; Schotter, J.; Bal, M.; Ursache, A.; Tuominen, M. T.; Stafford, C. M.; Russell, T. P.; Rotello, V. M. *Langmuir* **2001**, *17*, 6396–6398.
- (17) Li, Y.; Maire, H. C.; Ito, T. *Langmuir* **2007**, *23*, 12771–12776.
- (18) Landis, E. C.; Hamers, R. J. *J. Phys. Chem. C* **2008**, *112*, 16910–16918.

- (19) Szejtli, J. *Chem. Rev.* **1998**, *98*, 1743–1753.
- (20) Nijhuis, C. A.; Ravoo, B. J.; Huskens, J.; Reinhoudt, D. N. *Coord. Chem. Rev.* **2007**, *251*, 1761–1780.
- (21) Ju, H.; Leech, D. *Langmuir* **1998**, *14*, 300–306.
- (22) Matsue, T.; Evans, D. H.; Osa, T.; Kobayashi, N. *J. Am. Chem. Soc.* **1985**, *107*, 3411–3417.
- (23) Nielson, R. M.; Lyon, L. A.; Hupp, J. T. *Inorg. Chem.* **1996**, *35*, 970–973.
- (24) Rojas, M. T.; Koeniger, R.; Stoddart, J. F.; Kaifer, A. E. *J. Am. Chem. Soc.* **1995**, *117*, 336–343.
- (25) Kaifer, A. E. *Acc. Chem. Res.* **1999**, *32*, 62–71.
- (26) Pandey, B.; Tran Ba, K. H.; Li, Y.; Diaz, R.; Ito, T. *Electrochim. Acta* **2011**, *56*, 10185–10190.
- (27) Wimbush, K. S.; Reus, W. F.; van der Wiel, W. G.; Reinhoudt, D. N.; Whitesides, G. M.; Nijhuis, C. A.; Velders, A. H. *Angew. Chem., Int. Ed.* **2010**, *49*, 10176–10180.
- (28) Li, Y.; Ito, T. *Langmuir* **2008**, *24*, 8959–8963.
- (29) Godinez, L. A.; Schwartz, L.; Criss, C. M.; Kaifer, A. E. *J. Phys. Chem. B* **1997**, *101*, 3376–3380.
- (30) Lee, S. B.; Martin, C. R. *Chem. Mater.* **2001**, *13*, 3236–3244.
- (31) Lee, S. B.; Mitchell, D. T.; Trofin, L.; Nevanen, T. K.; Soderlund, H.; Martin, C. R. *Science* **2002**, *296*, 2198–2200.